Water SA 52(1) 82–96 / Jan 2026
https://doi.org/10.17159/wsa/2026.v52.i1.4197

Research paper

Physicochemical autopsy and sequential cleaning optimization of seawater reverse-osmosis membranes: a study from Beni Saf desalination plant, Algeria

Abdessalam Radjai[1], Mourad Amara[2,3], Fouzia Houma[1], Hafida Hadjar[4,5], Safia Chernai[1], Saifi Amirouche[4,6] and Boualem Hamdi[1]

[1]ENSSMAL, École Nationale Supérieure des Sciences de la Mer et de l'Aménagement du Littoral, BP 19 Campus Universitaire, Bois des Cars, Dely Ibrahim, 16320, Algiers, Algeria
[2]Laboratory of Hydrometallurgy and Molecular Inorganic, Chemistry, Faculty of Chemistry, USTHB, El Alia, BP 32, 16111, Algiers, Algeria
[3]National School of Nanoscience and Nanotechnology (ENSNN), Sidi Abdellah, Technological Hub, Algiers, Algeria
[4]CRAPC, Centre de Recherche Scientifique et Technique en Analyses Physico-Chimiques, BP 384, Zone Industrielle, Bou-Ismail, RP 42004, Tipaza, Algeria
[5]LPCMAE, Laboratoire d'Etude Physico-Chimique des Matériaux et Application à l'Environnement, Faculty of Chemistry, USTHB University, BP 32, El Alia Beb Ezzouar, 16111, Algiers, Algeria
[6]URMPE, Unité de Recherche, Matériaux, Procédés et Environnement, M'hamed Bougara University, Boumerdès, 35000, Algeria

This study focused on the fouling of two seawater reverse osmosis (SWRO) membranes at the Beni Saf Water Company desalination plant in Algeria, which has a daily capacity of 200 000 m^3 and a recovery rate of 45% using 17 920 membranes. Approximately 3 234 membranes are replaced annually due to fouling. A detailed study of the fouling agents of the two membranes was conducted using various analytical techniques, such as moisture analysis, loss on ignition (LOI), determination of calcium carbonate ($CaCO_3$) content, x-ray fluorescence (XRF), x-ray diffraction (XRD), and Fourier-transform infrared spectroscopy with attenuated total reflectance (FTIR-ATR). Surface characterization was also performed using scanning electron microscopy equipped with energy-dispersive x-ray spectroscopy (SEM-EDS), FTIR-ATR, and XRD. The LOI analysis indicated that more than 30% of the fouling material was organic in nature. FTIR-ATR identified the presence of –OH groups, phenolic C–O groups, and amide bonds, suggesting the accumulation of organic substances such as proteins, humic substances, and polysaccharides. Additionally, SEM-EDS, XRF, and XRD revealed relatively high concentrations of silica, primarily in the form of quartz, confirming the formation of an organo-inorganic complex on the membrane surface. Based on these findings, a sequential chemical cleaning protocol was developed, incorporating alkaline (NaOH), metal chelator (EDTA), surfactant (SDS), oxidant (H_2O_2), and sulfuric acid (H_2SO_4), each followed by rinsing with deionized water (DI). This cleaning regime effectively removed fouling from the membrane surface, resulting in an average weight loss of 15% for one membrane and 14% for the other.

CORRESPONDENCE
Abdessalam Radjai

EMAIL
abdesselam.radjai@enssmal.edu.dz

DATES
Received: 7 February 2025
Accepted: 10 December 2025

KEYWORDS
desalination
autopsy
membrane fouling
foulant characterization
chemical cleaning
Algeria

INTRODUCTION

North African countries face a critical water crisis driven by natural and human factors, resulting in alarmingly low freshwater availability (less than 1 000 m^3/inhabitant per year) (Leal Filho et al., 2022; Soula et al., 2021). Unsustainable water demand, fuelled by population growth, urbanization, and rising living standards (Gleick, 2014), is exacerbated by climate change, poor water network maintenance, and inadequate treatment infrastructure (Kusangaya et al., 2014). These challenges hinder socio-economic development and water security (Zlati et al., 2024). To address this crisis and achieve water and food security as part of sustainable development goals, governments must adopt innovative strategies, including non-conventional water resource treatment powered by renewable energy (Kusangaya et al., 2014; Al-Saidi et al., 2016). Among advanced desalination technologies (thermal, electrochemical, and reverse osmosis (RO)), RO membrane desalination stands out as the most promising, offering high-quality potable water while minimizing environmental impact (Lee et al., 2021).

North Africa and the Middle East dominate the global desalination market, representing 70% of its capacity (Philibert et al., 2024). Algeria, a regional leader, has constructed 21 desalination plants in less than 20 years, investing heavily in seawater desalination since 2000 (Mahmoudi et al., 2023). Today, Algeria ranks first in Africa and second in the Arab world (after Saudi Arabia) in desalinated water production capacity (Sayed et al., 2023). According to the National Statistics Office (ONS, 2024), Algeria's population reached 46.3 million in 2023, with projections of 47.4 million by 2024 and 52 million by 2030. This demographic growth, combined with ongoing drought conditions, has driven annual potable water demand to over 52 billion m^3. To combat these challenges, the government has invested heavily in desalination in a staggered development programme (as shown in Fig. A1, Appendix): (i) initial phase – 23 monobloc plants (57 500 m^3/day) and 14 large-scale plants (2.2 million m^3/day), providing 18% of potable water (Amitouche and Remini, 2016); (ii) second phase – 5 mega-plants (300 000 m^3/day each) entered service in 2025, increasing desalinated water's share to 42% of the country's drinking water production and total capacity to 3.7 million m^3/day; (iii) third phase: 7 new plants by 2027, including 6 plants treating 300 000 m^3/day and one 60 000 m^3/day plant, raising total capacity to 5.61 million m^3/day. To oversee these efforts, Algeria established the

National Desalination Agency (ANDE) in 2023 (JORA, 2023). This agency is responsible for the completion, operation, and maintenance of desalination plants and related infrastructure, ensuring efficient and effective performance.

The rapid deployment of membrane-based seawater desalination plants has led to frequent technical shutdowns, primarily due to membrane fouling, causing significant financial losses and water distribution disruptions. These issues are exacerbated by poorly located plants near polluted areas, such as river mouths with high suspended solids and industrial spills. Poor seawater quality, inadequate pre-treatment, and marine hydrodynamics contribute to premature fouling, reducing potable water production by over 40% in some cases. Under optimal conditions, RO membranes are typically replaced every 2–3 years to maintain efficiency (Choi et al., 2009; Khoo et al., 2021). However, in some Algerian plants, membrane lifespans are less than 2 years, influenced by raw water quality, hydraulic conditions, fouling, and cleaning frequency (Ahmed et al., 2023). Premature replacements increase costs and disrupt operations.

The Beni Saf Water Company plant in Algeria, has a capacity of 200 000 m^3 per day, consuming an average of approximately 3 234 membranes annually (18% of its total). Across Algeria's 21 desalination plants (producing 2.26 million m^3/day), around 15 000–25 000 membranes are replaced yearly, resulting in an estimated 8–12 million USD in annual losses. Despite the significant impact of premature fouling, systematic studies on this issue are lacking. Membrane autopsies are essential to diagnose fouling causes and inform decision-making.

By foulant class, 4 types dominate: organic, colloidal, biofouling, and mineral scaling. Organic fouling (NOM: humic acids/fulvic acids, proteins, polysaccharides) is strongly influenced by pH and divalent cations; lower pH and higher Ca^{2+}/Mg^{2+} enhance adsorption/bridging and flux decline, and hydrophobic/rough surfaces foul more readily (Yang et al., 2021; Hong and Elimelech, 1997). Scaling increases with recovery as sparingly soluble salts exceed solubility at the surface; severity depends on supersaturation and precipitation kinetics and is exacerbated by concentration polarization (common scales: $CaCO_3$, $CaSO_4$, $BaSO_4$, Ca-phosphate, silica) (Jawor and Hoek, 2009; Matin et al., 2019). Biofouling begins with a NOM followed by microbial attachment; biofilms thicken with nutrients and can become partially irreversible, causing flux loss, differential pressure (ΔP) rise, and occasional membrane biodegradation (Creber et al., 2010; Matin et al., 2011; Flemming, 1997). Colloidal fouling (1–1 000 nm; silt, silica, clays, iron oxides, macromolecules) is often tracked by SDI/turbidity and typically proceeds via cake-enhanced concentration polarization, which raises near-surface osmotic pressure and reduces driving force (Adel et al., 2022; Al-Amoudi and Lovitt, 2007).

This study aimed to conduct a detailed physicochemical autopsy of fouling on two SWRO membranes from the Beni Saf Water Company (BWC) desalination plant in Algeria, identifying the primary fouling agents. The results should help the plant operator improve management of operations. To achieve this goal, a comprehensive analysis of the extracted fouling material was performed using various techniques, including moisture analysis, loss on ignition (LOI), determination of $CaCO_3$ percentage, Fourier-transform infrared spectroscopy with attenuated total reflectance (FTIR-ATR), x-ray diffraction (XRD), and x-ray fluorescence (XRF). Additionally, the membrane surface was also examined using scanning electron microscopy equipped with energy-dispersive x-ray spectroscopy (SEM-EDS), FTIR-ATR, and XRD.

MATERIAL AND METHODS

Description of the Beni Saf Water Company (BWC) plant

The BWC plant is located in the Aïn Témouchent Province on the coast of the Alboran Sea. It serves the water needs of two provinces suffering from limited access to freshwater resources. The plant's flow diagram (Fig. 1) illustrates the various stages of the desalination process. The RO unit consists of 10 racks, each rack containing 265 tubes, with 7 membrane elements installed per tube. A total of 17 920 Hydranautics-SWC5-MAX RO membranes produce a total daily capacity of 200 000 m^3.

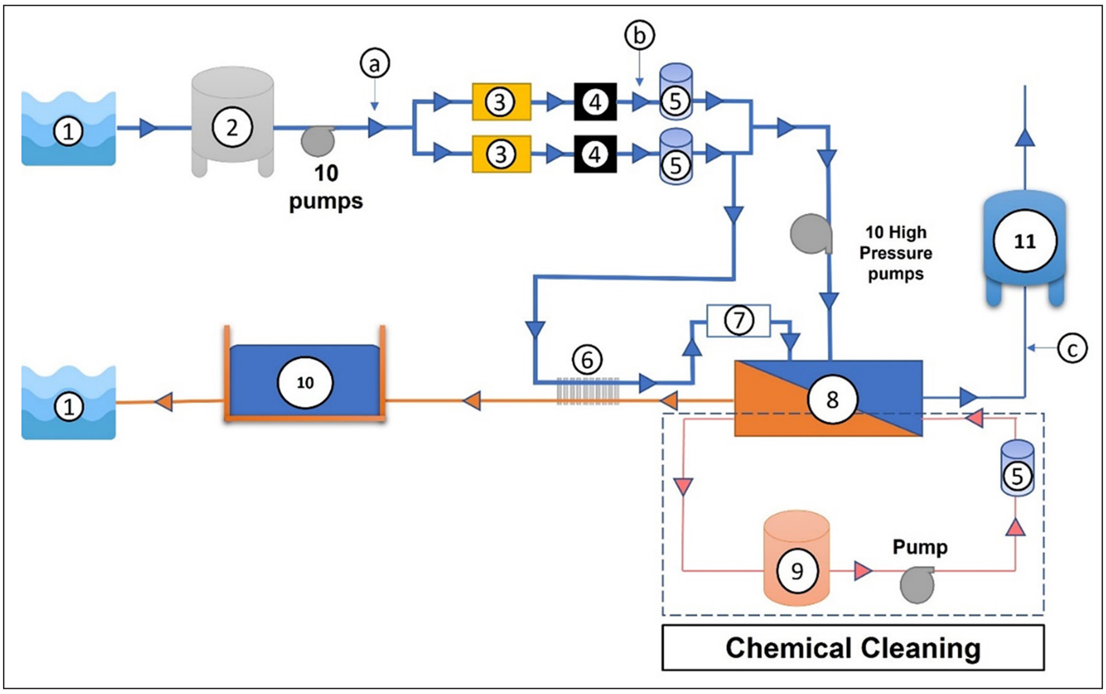

Figure 1. Flow diagram of BWC reverse osmosis desalination plant: 1 – seawater; 2 – catchment tank; 3 – sand filter; 4 – anthracite filter; 5 – cartridge filter; 6 – ERI energy recovery; 7 – booster pump; 8 – reverse osmosis racks; 9 – chemical tank; 10 – brine tank; 11 – expedition tank; a – ferric chloride; b – sodium bisulfite + antiscalant; c – CO_2, calcite, and sodium hypochlorite

Seawater is abstracted at a fixed intake tower located approximately 1.2 km offshore, with the intake ports positioned 5 m below the water surface. From the tower, water flows by gravity through a submarine polyethylene pipeline (diameter 2 400 mm) to the onshore catchment tank. The main physicochemical characteristics of seawater around the intake tower are summarized in Table 1. Most measurements are from a single sampling campaign (July 2024); SDI values are 1-year averages.

Membranes and fouling material sampling and preparation

Two Hydranautics SWC5-MAX elements (Memb01 and Memb02) from Rack No. 10 at the BWC plant were removed for autopsy; each occupied the No. 2 position in different pressure vessels. Elements were taken from the second position rather than the first to avoid lead-element bias from transient high turbidity events and operational anomalies, while still capturing a fouling profile representative of normal plant operation. Removal was prompted by a rack-specific 19% decrease in normalized permeate production, coincident with a progressive rise in rack ΔP, indicative of fouling; this decline does not reflect plant-wide performance. This sampling was designed to identify the plant's dominant fouling type. The membranes were visually inspected for physical deterioration, dissected to remove the outer casing, and unfolded for layer-by-layer examination. From each selected fouling layer, 9 square-shaped coupons (3 cm × 3 cm) were systematically cut from visibly fouled areas (Fig. 2). Two sample types were collected: (i) membrane coupons: the 3 cm × 3 cm coupons were cut from the fouled area; (ii) fouling material: remaining foulants on the membrane surface were carefully scraped and stored in Petri dishes (Díaz Salazar and Gorczyca, 2024). Both membrane coupons and fouling material samples were stored at 4°C for further analysis.

Membranes and fouling material characterization

To study the fouling material scraped up from the two membranes, several parameters were measured. Moisture content was determined by weighing the samples before and after drying at 105°C for 24 h. LOI was performed by incinerating the samples at 525°C for 4 h to estimate the percentage of organic matter (OM) (Fu et al., 2020; Heiri et al., 2001). $CaCO_3$ content was determined using Bernard's calcimeter through acid digestion, with CO_2 release measured according to the French AFNOR standard (AFNOR, 1996). Semi-quantitative XRF analyses were conducted on a SciAPS apparatus to determine the elemental composition of inorganic substances present. The crystalline structure of inorganic compounds was characterized by XRD using a BRUKER D8 Advance with CuKα radiation. The morphology and surface

Table 1. Water quality at the BWC SWRO plant (seawater, before cartridge filter, before RO)

Parameters	Units	Seawater	Before CF	Before RO
Temperature	°C	25.9 ±0.3	23.30 ±0.4	23.40 ±0.3
pH	-	8.14 ±0.02	8.14 ±0.02	8.13 ±0.04
Turbidity	NTU	0.16 ±0.01	0.18 ±0.01	0.13 ±0.02
Conductivity	mS/cm	58.70 ±0.05	52.40 ±0.07	52.70 ±0.09
Dissolved oxygen	mg/L	5.80 ±0.09	4.40 ±0.12	4.40 ±0.3
TDS	mg/L	41 000	36 000	36 700
Suspended solids	mg/L	78.00 ±0.90	35.80 ±1.30	14.70 ±0.70
Particulate organic matter	mg POM/L	32.16 ±1.60	38.36 ±2.20	27.89 ±1.40
Hardness as $CaCO_3$	mg $CaCO_3$/L	7 030	7 005	6 800
Alkalinity	mg/L	195 ±35	190.65 ±21	185.17 ±26
NO_3^-	µg/L	03.55	03.14	03.47
NO_2^-	µg/L	01.46	01.68	01.86
PO_4^{3-}	µg/L	56.14	72.17	88.30
SiO_2	µg/L	81.14	66.01	50.88
Total plate count at 22°C/48 h	cfu/100 mL	133	0	0
SDI after cartridge filter	-	-	-	1.8

CF: cartridge filter; RO: reverse osmosis; ND: not analysed

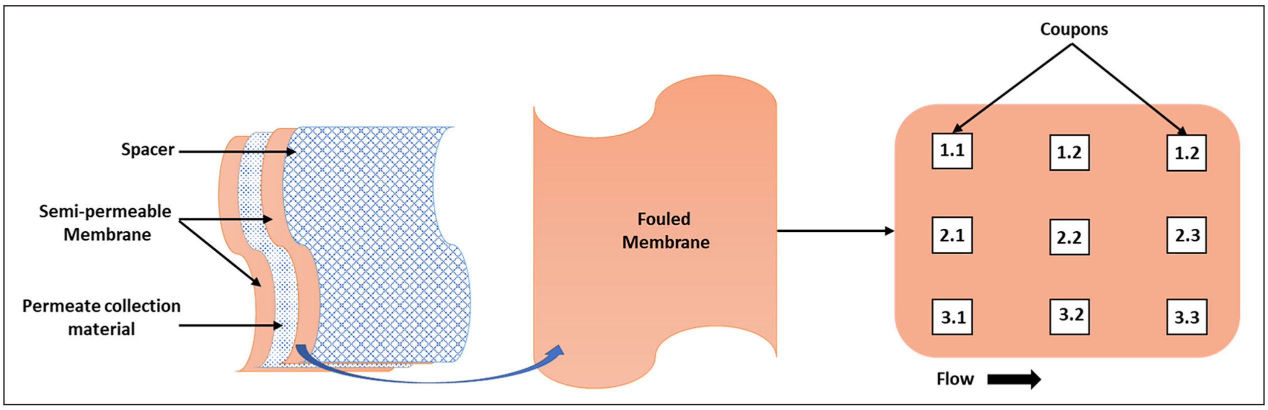

Figure 2. Sampling and cutting of coupons from fouled surface layers

composition were studied using SEM-EDS, respectively, on a Zeiss Smart SEM EDX system. FTIR-ATR was performed using an Alpha-Bruker spectrometer, operating in the 4 000–300 cm^{-1} wavenumber range at a 2 cm^{-1} resolution, to identify the specific functional groups present in the fouling material. The coupons from both membrane modules were also characterized by SEM-EDS. The SEM provided detailed images of the membrane surface, while EDS identified the elemental distribution of the remaining fouling material. Additionally, FTIR-ATR and XRD were used to analyse the functional groups and crystalline phases of the close surface deposits.

Chemical cleaning

Several studies (Filloux et al., 2015; Gul et al., 2021; Unal, 2022; Wang et al., 2015) have explored the effectiveness of various cleaning agents by immersing membrane coupons in different solutions to evaluate their capacity to remove fouling under controlled conditions. A comprehensive examination was conducted with a range of chemical agents, including alkaline agents (sodium hydroxide, NaOH; potassium hydroxide, KOH), acids (hydrochloric acid, HCl; acetic acid, CH_3COOH; sulfuric acid, H_2SO_4), surfactant (sodium dodecyl sulfate, SDS), chelating (ethylenediaminetetraacetic acid, EDTA), and oxidizing (hydrogen peroxide, H_2O_2) agents. Each agent was evaluated for its cleaning potential. After accurate preparation of chemical cleaning solutions was completed, the effectiveness of the cleaning process was assessed by exposing small coupons (4 cm^2) cut separately from various areas of the fouled membranes to the following steps:

- Preparation of the chemical solutions
- Precise weighing and photography
- Immersion in 70 mL of each cleaning solution
- Agitation for 6 h at a controlled temperature
- Drying at 40°C for 48 h
- Weighing after cleaning to determine the residual mass
- Post-cleaning photographing to document any changes in colour and/or aspect

Following the initial cleaning process, the selection of suitable agents for sequential cleaning was based on comparing observed weight loss and changes in the membrane colour. A series of sequential cleaning tests were conducted to establish the most effective chemical cleaning regimen.

RESULTS AND DISCUSSION

Visual inspection

Visual inspection of the fouled membranes revealed no noticeable physical damage. A systematic examination of each layer confirmed this observation, alleviating concerns about performance degradation due to structural alterations. Optical images of the fouling on Memb01 and Memb02 (Fig. 3) show a gradual accumulation of dark brown gelatinous deposits, with a concentration gradient along the flow path. This likely results from complexes formed between humic acids and iron, creating a gelatinous brown layer (Nyström et al., 1996). Fouling was most severe at the flow inlet, diminishing toward the outlet. The significant deposits indicate substantial fouling on both membranes (Fig. 3).

Characterization of fouling material

Moisture content, LOI, and $CaCO_3$

The moisture content was approximately 2% for Memb01 and 1.62–3.18% for Memb02, likely due to the presence of fine particles, such as clays, known for their hydrophilic properties (Paul and Naidu, 2022). Generally, residual moisture typically increases with higher clay and OM content (Baize, 2018). For external context, clayey textures commonly show 4–8% residual moisture, whereas sandy horizons can be <1%; our measurements for both membranes are within the low single-digit range, consistent with a mixed salt–clay–organic matrix (Baize, 2018). LOI analysis showed an average presence of 34.36% OM in the fouling of the first membrane and 32.44% in the second (Fig. 4). This OM content is likely due to the formation of organo-inorganic complexes during the desalination process (Baize, 2018).

Scaling from $CaCO_3$ can occur in nearly all types of feedwaters, including seawater, and can form resistant deposits on membrane surfaces (Tzotzi et al., 2007). However, $CaCO_3$ represented only 4% of the total fouling material in both membranes (Fig. 4), suggesting effective anti-scalant dosage upstream of the cartridge filters or removal during acid-based cleaning (pH 2.5–3.5).

FTIR-ATR analysis of fouling material

Analysis of the fouling materials from both membranes (Fig. 5) revealed distinct peaks at specific wavenumbers.

FTIR-ATR analysis (Table 2) indicates that fouling is predominantly organic in both membranes, derived from POM in seawater (Table 1). Peaks associated with hydroxyl groups, phenolic compounds, amide bonds, and C–C bonds suggest the accumulation of rubber proteins, humic substances, and polysaccharides. Inorganic fouling, indicated by SiO_2 peaks, results from Si-based mineral deposits. Memb01 and Memb02 share the same set of diagnostic bands, indicating the same foulant classes. However, band depths differ between the spectra – several features are more pronounced on Memb01, whereas others are stronger on Memb02. Because band positions coincide and the spectra were compared, these intensity differences are attributed to the relative concentration of the same organic functionalities, rather than different chemistries. Overall, the deposits comprise a mixed organic–inorganic layer.

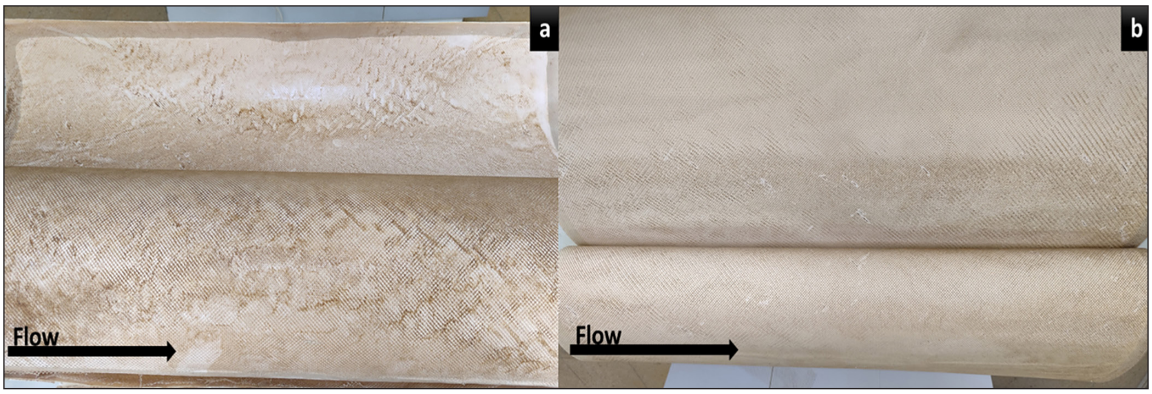

Figure 3. Visual inspection of both membranes: (a) Memb01, (b) Memb02

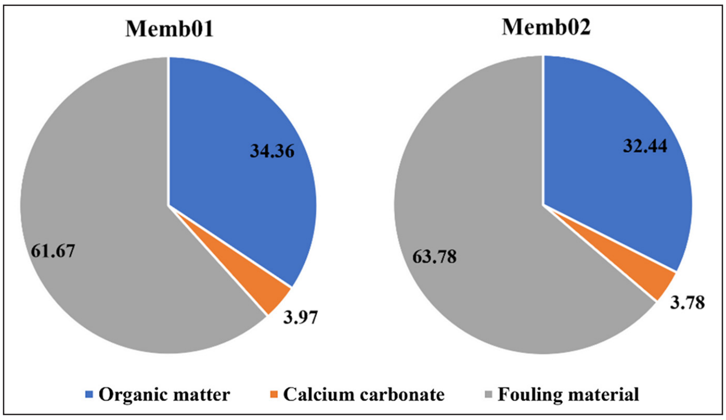

Figure 4. Percentage of OM and $CaCO_3$ in the fouling materials of both membranes

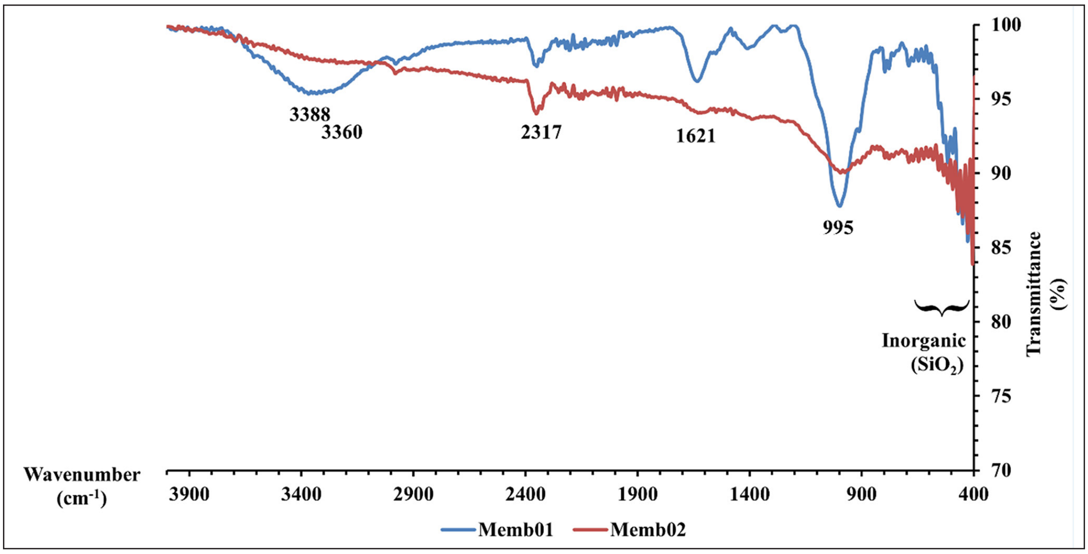

Figure 5. ATR-FTIR spectra of Memb01 and Memb02 fouling materials

Table 2. FTIR-ATR analysis of fouling materials

Wavenumber (cm^{-1})	Assignment	Potential compounds/sources	References
3 360–3 388	–OH hydroxyl groups	Polysaccharides, humic substances, free/bonded NH groups	Hasanzadeh et al. (2023) Wu et al. (2015) Veerasamy and Ismail (2012)
2 317	Water molecule bond deformation	Water	Khalil et al. (2024)
1 621	C=O stretching (amide I bonds)	Rubber protein-like materials derived from latex	Pan et al. (2017) Liu et al. (2016)
1 255	C–O stretching vibrations (phenolic compounds)	Phenolic compounds (faint signal)	Mokhtari et al. (2017) Ren et al. (2015)
1 082 and 796	Si–O–Si stretching vibrations	Inorganic Si-based compounds (e.g., SiO_2)	Hussein Al-Timimi et al. (2022) Goh et al. (2018)
401–455	SiO_2 vibrations	Inorganic Si-based compounds	Tapiero et al. (2023)
995	C=O functional groups	Accumulated polysaccharides	Adel et al. (2022)

XRF investigation of deposited fouling material

To evaluate longitudinal variability, fouling material was scraped at the inlet, middle, and outlet of each membrane and analysed by XRF. The results (Table 3) showed that Si, Al, and Fe were the predominant metallic elements in the fouling materials of both membranes. Minor elements (S, P, K, Ca, Ti, Cu) had a total concentration below 2%, while trace elements (Mn, Ni, Zn, As, Rb, Sn, Cr, Mo, Co, Sr, Nb, Zr) had a combined concentration of less than 0.2%. Collectively, these findings indicate minimal contributions from inorganic colloids and metal oxides to fouling, thereby confirming a common fouling type. The high concentrations of Si and Al indicate that clay minerals may play a role in fouling (Leger and Hawker, 1987). Prolonged operation could lead to the accumulation of insoluble aluminosilicate deposits (Melián-Martel et al., 2012). Most heavy metals are likely by-products of nearby industrial activities (Kabata-Pendias and Mukherjee, 2007), particularly discharges from the Beni Saf cement factory near the desalination plant. Across positions, Memb02 exhibited higher inorganic fractions than Memb01. These results indicate that inorganic foulants are primarily captured at the inlet part of the elements, while the observed differences reflect differences in concentration rather than a change in composition.

Table 3. Chemical composition of inorganic elements in fouling material scraped from both RO membranes, determined by XRF

Element	Concentration (%)					
	Memb01			Memb02		
	Inlet	Middle	Outlet	Inlet	Middle	Outlet
Al	1.740 ±0.035	2.150 ±0.037	1.850 ±0.035	3.950 ±0.047	2.820 ±0.047	2.050 ±0.038
Si	4.040 ±0.026	4.760 ±0.028	3.450 ±0.024	13.530 ±0.045	7.440 ±0.038	4.170 ±0.027
Fe	1.300 ±0.009	1.190 ±0.009	1.350 ±0.009	1.930 ±0.013	1.460 ±0.010	1.290 ±0.009
S	0.452 ±0.004	0.150 ±0.003	0.160 ±0.003	0.441 ±0.005	0.325 ±0.005	0.231 ±0.004
P	0.074 ±0.003	0.086 ±0.004	0.054 ±0.003	0.179 ±0.006	0.121 ±0.005	0.104 ±0.004
K	0.320 ±0.002	0.371 ±0.003	0.260 ±0.002	0.742 ±0.004	0.464 ±0.004	0.351 ±0.003
Ca	0.534 ±0.003	0.336 ±0.002	0.264 ±0.002	0.831 ±0.004	0.540 ±0.003	0.337 ±0.002
Ti	0.118 ±0.009	0.106 ±0.008	0.110 ±0.008	0.230 ±0.014	0.129 ±0.010	0.110 ±0.008
Mn	0.029 ±0.002	0.031 ±0.002	0.038 ±0.002	0.054 ±0.003	0.047 ±0.003	0.044 ±0.002
Ni	0.006 ±0.001	0.004 ±0.001	0.004 ±0.001	0.007 ±0.001	0.004 ±0.001	0.005 ±0.001
Cu	0.187 ±0.002	0.053 ±0.001	0.117 ±0.002	0.159 ±0.003	0.042 ±0.001	0.173 ±0.002
Zn	0.092 ±0.001	0.028 ±0.001	0.057 ±0.001	0.079 ±0.002	0.022 ±0.001	0.083 ±0.001
As	0.005 ±0.001	0.004 ±0.001	0.005 ±0.001	0.006 ±0.001	0.005 ±0.001	0.005 ±0.001
Rb	0.009 ±0.001	0.008 ±0.001	0.010 ±0.001	0.011 ±0.001	0.010 ±0.001	0.009 ±0.001
Sn	0.008 ±0.001	0.003 ±0.001	0.003 ±0.001	0.004 ±0.001	0.005 ±0.001	0.008 ±0.002
Cr	0.020 ±0.002	0.014 ±0.002	0.015 ±0.002	0.034 ±0.003	0.021 ±0.003	0.019 ±0.002
Mo	0.002 ±0.001	0.001 ±0.001	0.001 ±0.001	0.002 ±0.001	0.002 ±0.001	0.001 ±0.001
Co	0.007 ±0.002	-	0.007 ±0.001	0.009 ±0.003	0.007 ±0.002	0.006 ±0.002
Sr	0.008 ±0.001	0.007 ±0.001	0.008 ±0.001	0.010 ±0.01	0.010 ±0.001	0.008 ±0.001
Nb	0.001 ±0.001	0.001 ±0.001	0.001 ±0.001	0.001 ±0.001	0.001 ±0.001	0.006 ±0.001
Zr	-	0.006 ±0.001	0.005 ±0.001	0.012 ±0.001	0.010 ±0.001	0.005 ±0.001
Mg	-	-	0.160 ±0.001	-	1.710 ±0.376	-
Total (%)	8.950	9.309	7.769	22.221	14.485	9.015

XRD analysis of foulant material

XRD analysis of fouling material from both membranes revealed several peaks (Fig. 6), with diffraction angles at 20.87°, 26.61°, 31.70°, 39.42°, 45.58°, 50.16°, 60.00°, and 68.28°.

According to Khamis and Arafah (2017), the sharp peaks at 20.87°, 26.61°, 50.16°, 60.00°, and 68.28° indicate the presence of crystalline quartz (SiO_2), which typically originates from marine sediments. These results suggest that the inorganic component of the fouling material contains a significant amount of marine-derived quartz. Additionally, the peaks at 31.70° and 45.58° are attributed to NaCl, a residual salt from seawater, as identified by Al-Abri et al. (2022). The smaller peak at 39.42° corresponds to $CaCO_3$ (Sahadat Hossain et al., 2023), and the relatively low concentration of $CaCO_3$ in the fouling material aligns with the results from the Bernard calcimetry analysis, confirming the effectiveness of the anti-scalant used prior to cartridge filtration (Laqbaqbi et al., 2017).

Membrane surface characterization

SEM-EDS analysis of fouled membrane surface

The fouled membrane surfaces were analysed using SEM-EDS (Fig. 7). A thick and heterogeneous fouling layer was observed embedded with white particles, which could significantly impact permeate flow and potentially cause membrane deformation over time (Unal, 2022). Irregular particles were concentrated in the upper regions of the fouling layer; qualitative visual inspection indicated that their apparent density increased from the membrane inlet toward the outlet. Notably, white deposits larger than 100 µm and particles exceeding 5 µm were observed, despite pretreatment with cartridge filters before RO.

EDS analysis detected various elements in the fouled membranes, as shown in Fig. 8. The presence of C and O indicates an organic or biologically introduced contamination, while elements such as Na, Cl, Mg, Al, Si, K, Mo, Fe, and Ca suggest inorganic colloids and crystals (Lee et al., 2021; Adel et al., 2022). Ti, Nb, and S were also observed in some samples. Both membranes exhibited high levels of carbon (30–39%) and oxygen (38%) (Fig. 8), strongly suggesting organic fouling, such as from humic-like substances (Lee et al., 2021). The consistent carbon content (32%) aligns with LOI results.

Na and Cl, even at low percentages, likely originate from seawater, indicating NaCl deposition. Ca and S suggest potential scale formation (e.g., $CaCO_3$ and $CaSO_4$) (Butt et al., 1997). K and Ti further highlight the diversity of inorganic fouling.

Low percentages of Si, Al, Mg, and Fe suggest complex forms such as quartz or metallic silicates (e.g., Fe_2SiO_4, Al_2SiO_5, Mg_2SiO_4) (Adel et al., 2022). Their formation may be influenced by anti-scalants and sodium bisulfite (SBS) (Fortunato et al., 2020). Mo is likely from wastewater discharges of the nearby Beni Saf cement plant, as industrial facilities often release Mo residues (Gao et al., 2020). This underscores the impact of external sources, particularly industrial activities, on fouling characteristics.

Apparent differences in wt% between the two elements are consistent with non-uniform deposit thickness/packing and axial transport, rather than different chemistries. These variations also reflect characteristics of SEM-EDS: it is surface-sensitive and semi-quantitative, and signals are influenced by local heterogeneity of the fouled layer (Ahmed et al., 2023). Accordingly, the EDS data are interpreted qualitatively and indicate that both membranes experienced the same fouling type; differences in concentration reflect the extent and spatial distribution of the same foulant classes (Martin et al., 2014).

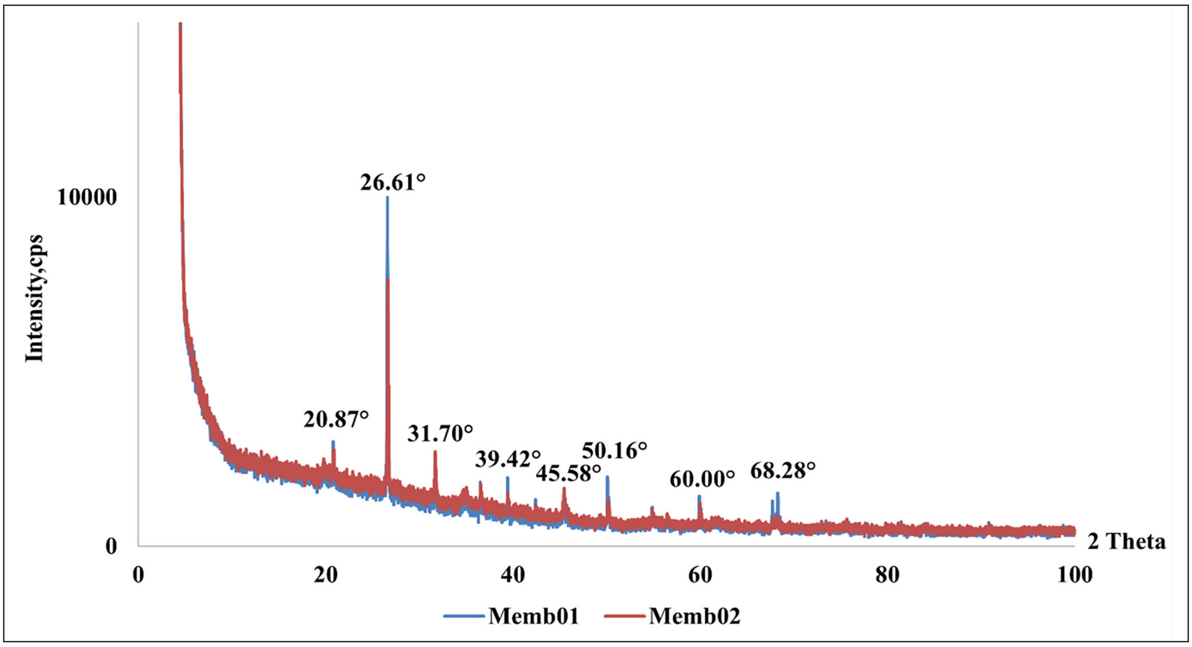

Figure 6. XRD pattern of foulant material deposited on SWRO membranes

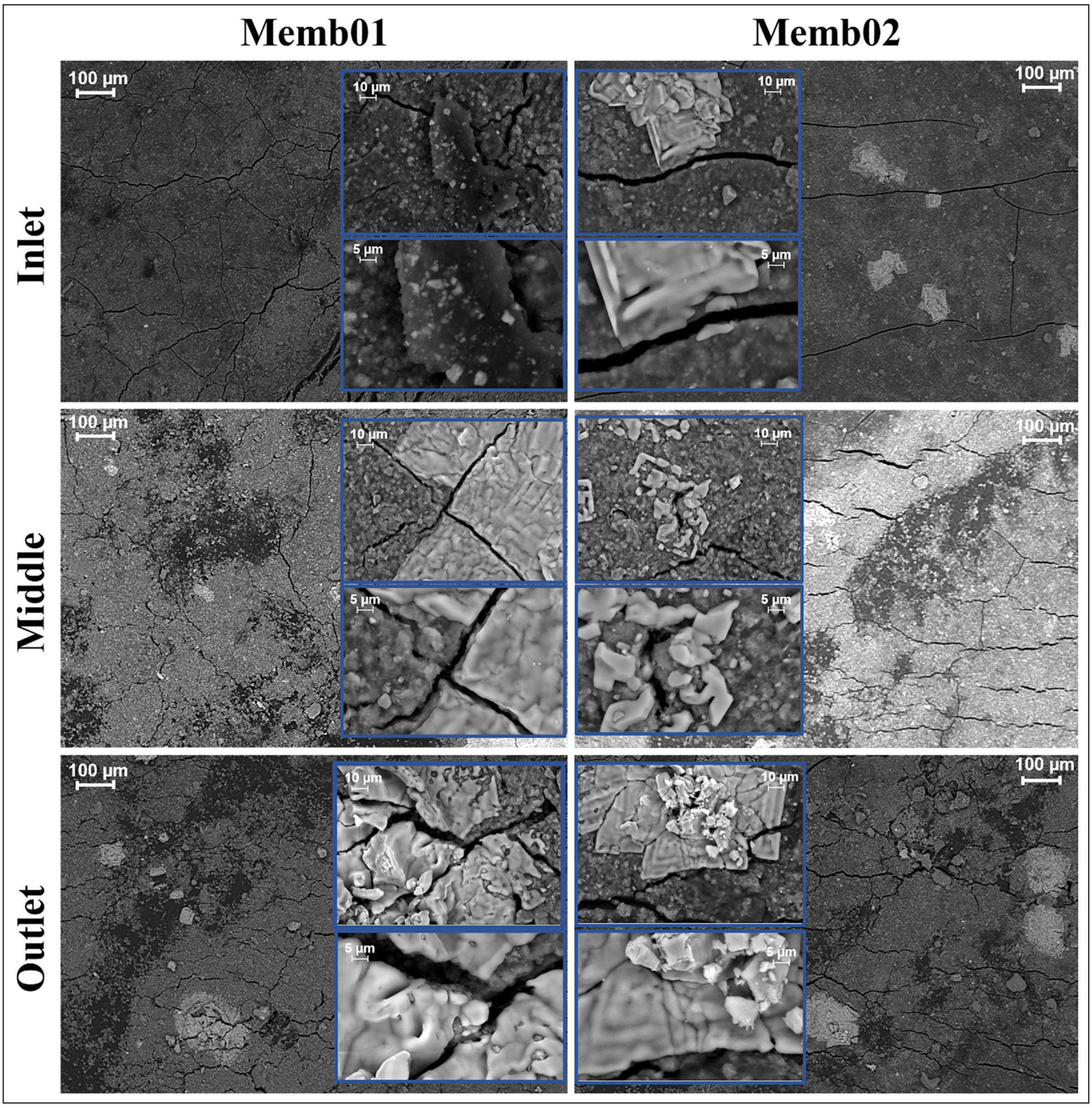

Figure 7. SEM images of the fouled SWRO membrane at inlet, middle, and outlet sections

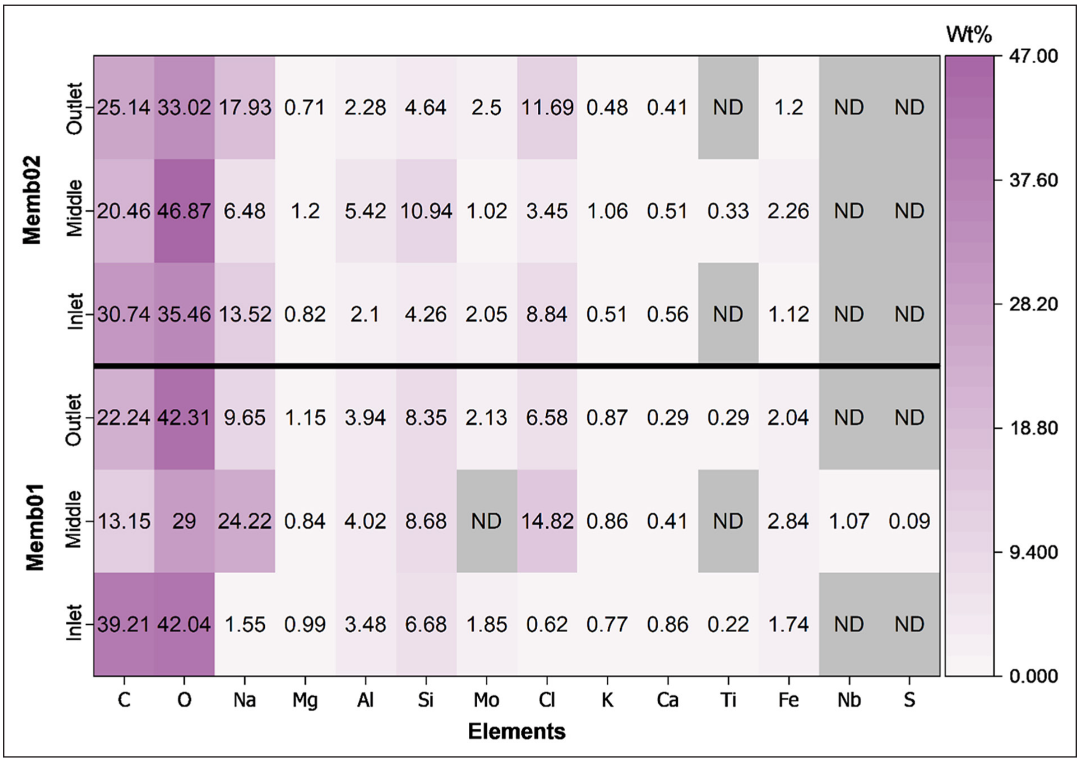

Figure 8. Heatmap of elemental composition of fouling on SWRO membranes determined by EDS; Wt% – weight; ND – not detected

FTIR-ATR spectral analysis of fouled membrane surface

The FTIR-ATR spectra from both membrane surfaces revealed several peaks that provide insight into the composition of the fouling material (Fig. 9). The most significant peaks observed are mentioned in Table 4.

The two membranes show similar band sets; several peaks appear stronger on Memb01, consistent with differences in areal coverage and concentration of the fouling material, and with the qualitative nature of ATR-FTIR. Thus, both Memb01 and Memb02 exhibit the same foulant classes, while intensity differences reflect the extent and spatial distribution of those classes.

The analysis reveals that fouled membranes consist of both organic and inorganic components. Organic fouling, derived from POM in seawater, dominates, while inorganic fouling results from mineral deposits.

The band assignments on the membrane surfaces (phenolic, amide, aromatic features, and carbonate) align with those observed for the scraped fouling material in Table 2, including Si–O–Si and broad O–H signatures. This concordance indicates that both approaches identify the same organic-dominated fouling with an inorganic contribution (silica/silicate and minor carbonate).

XRD investigation of membrane surface

The XRD patterns (Fig. 10) of the membrane coupons (Memb01 and Memb02) show peaks in the 2θ range of 15° to 30°, along with peaks similar to those observed in the fouling material.

For Memb01, peaks were identified at 26.96°, 31.64°, 45.56°, 50.13°, and 60.20°. Memb02 presented peaks at 26.47°, 31.69°, 45.50°, 50.36°, 60.08°, and 68.32°. The peaks in the range 2θ = 15–30° are characteristic of the amorphous nature of polyamide membranes, as previously reported by Melián-Martel et al. (2012). Additional peaks observed in both membrane coupons, which closely align with those identified in the fouling material, reaffirm the presence of SiO_2, NaCl, and traces of $CaCO_3$, as noted earlier.

Chemical cleaning

Single chemical agent cleaning tests

The experiment aimed to evaluate the effectiveness of 8 different chemical agents for cleaning fouled membranes. The concentrations of the agents were as follows: NaOH (0.1 N), KOH (0.1 N), HCl (0.1 N), acetic acid (0.1 N), sulfuric acid (0.1 N), SDS (10 mM), EDTA (1 mM), and H_2O_2 (1 N). The membrane coupons were agitated in these solutions for 6 h, dried, and their weight loss (Fig. 11) and colour changes recorded.

The use of NaOH and KOH at 0.1 normality led to significant colour changes in the fouling of both membranes, especially with NaOH, which resulted in a 12% weight loss (Fig. 11). The alkaline agents raise the solution's pH, increasing the negative charge density of organic foulants through carboxyl group deprotonation, enhancing foulant solubility (Ahmed et al., 2023).

No significant colour changes were observed in membrane fouling for the acidic agents, including HCl, sulfuric acid, and acetic acid, and the weight loss was negligible. Acidic cleaning is typically employed to remove precipitated salts or scales, such as $CaCO_3$ (Lin et al., 2010). The relatively low percentage of $CaCO_3$ identified in the fouling material confirms that acid cleaning was less effective due to the minor role of scaling in the fouling of these membranes.

Both EDTA and SDS showed effectiveness in removing fouling material from the membrane surfaces (Ang et al., 2006). SDS's ability to clean RO membranes fouled by OM has already been reported (Hong and Elimelech, 1997).

At pH 11, H_2O_2 effectively removed fouling by oxidizing NOM into more oxygenated functionalities (carboxyl, ketonic, aldehydic) that, under alkaline conditions, are deprotonated and more susceptible to base-catalysed hydrolysis, increasing hydrophilicity and solubility (Kramer et al., 1984; Porcelli and Judd, 2010). This supports the superior cleaning efficiency of combined oxidants and alkaline agents over oxidants alone, especially for organic fouling.

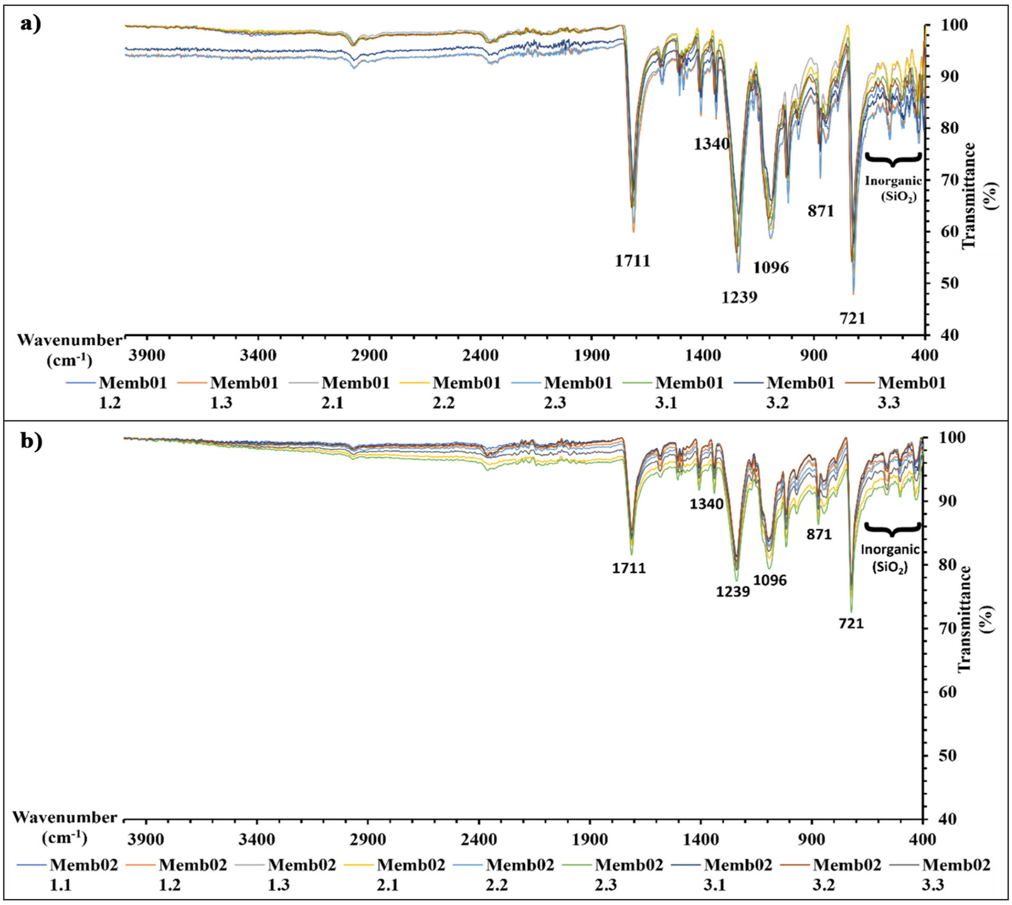

Figure 9. FTIR spectra of fouled coupons from both SWRO membranes: (a) Memb01; (b) Memb02

Table 4. FTIR-ATR analysis of membrane surface

Wavenumber (cm^{-1})	Assignment	Potential compounds/sources	References
1 711	Aromatic amide bonds	Proteins	Jung et al. (2018) Tapiero et al. (2023)
1 340	O–H stretching vibrations in carboxyl groups (–COOH)	Humic substances	Liu et al. (2024)
1 239	DNA/RNA/free phosphate/ phospholipid (P=O)	Biological	Khan et al. (2014) Ahmed et al. (2023)
1 096	Alkoxy groups	Humic acid	Hansima et al. (2022)
871	Carbonates	$CaCO_3$ crystals	Karmal et al. (2020) Unal (2022) Ahmed et al. (2023)
721	C–H stretching (aromatic skeleton)	Aromatics in humic substances	Ashfaq et al. (2019) Thygesen et al. (2014) Smith (2018) Tran et al. (2007) Adel et al. (2022)
1 583	COO^- stretching bands	Proteins, polysaccharides, amino sugars	Sakinah et al. (2007) Thygesen et al. (2014)
1 503	C=C stretching vibrations in aromatic rings	Polysulfones	Thuvander et al. (2018) Tapiero et al. (2023) Fontyn et al. (1991)
1 487	Aromatic pyridine ring, aliphatic C-O bond deformation	Organic compounds	Shafi et al. (2017)
1 408	–COO– stretching vibrations	Carboxylic acids, humic acid	Fan et al. (2024) Zheng et al. (2018)
1 016	Symmetrical C–O–C stretching	Organic compounds	Pulyalina et al. (2022)
969	Phosphate group (P–O)	Biological materials	Liu et al. (2013)
845	Symmetrical C–O–C stretching	Diethyl ether	Smith (2018)
792	Asymmetric C–N–C stretching (tertiary amides)	Organic compounds	Lamsal et al. (2012)
559	SO_2 group	Inorganic compounds	Guo et al. (2019) Pihlajamäki et al. (1998)
500–400	Inorganic substances	SiO_2	Tapiero et al. (2023)

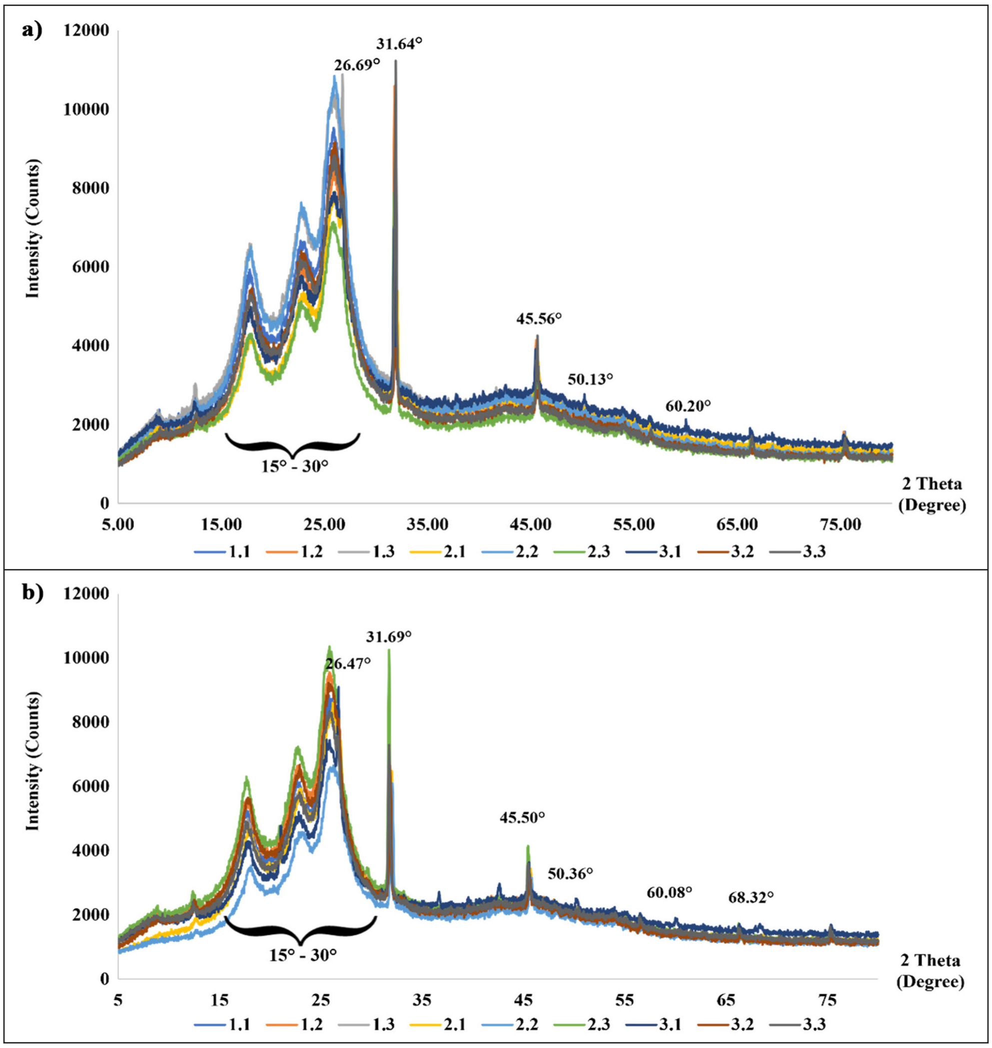

Figure 10. XRD patterns of fouled SWRO membranes: (a) Memb01; (b) Memb02

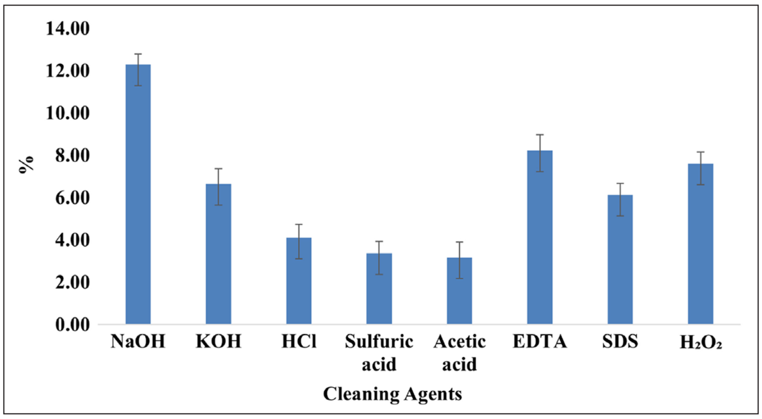

Figure 11. Percentage of mass loss of fouling material for each cleaning agent

Sequential cleaning

Based on the comprehensive analysis of the fouling material's composition and the effectiveness of chemical agents, the key to effective membrane cleaning lies in the successful removal of OM. Vendor guidance recommends avoiding low-pH cleaning initially, as it could worsen organic fouling by solidifying OM (Hydranautics, 2014). The literature indicates that alkaline cleaning is more effective than acidic cleaning for organic fouling because alkaline agents promote OM hydrolysis and solubilization (Madaeni and Samieirad, 2010). A sequential cleaning regimen, starting with SDS, followed by EDTA, proved highly effective for membranes fouled with OM under alkaline conditions (Al Ashhab et al., 2017). In addition, H_2O_2 at high pH degrades NOM functional groups, making them more susceptible to hydrolysis (Kramer et al., 1984; Porcelli and Judd, 2010). By contrast, acidic cleaning is most effective for removing precipitated salts (Gan et al., 1999). Prior work also reports that combining NaOH and SDS, followed by acidic treatment, effectively regenerates membranes (Madaeni and Samieirad, 2010).

Guided by the above, we devised a sequential approach using agents tailored to OM removal and subsequent scale removal. The chosen agents included deionized water (DI), NaOH (pH = 12),

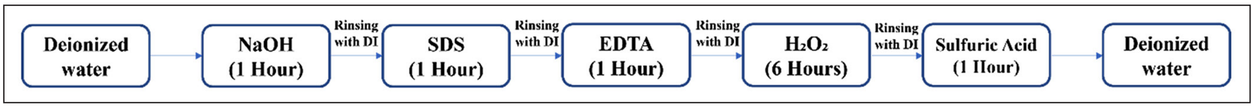

Figure 12. Sequential cleaning of membrane coupons

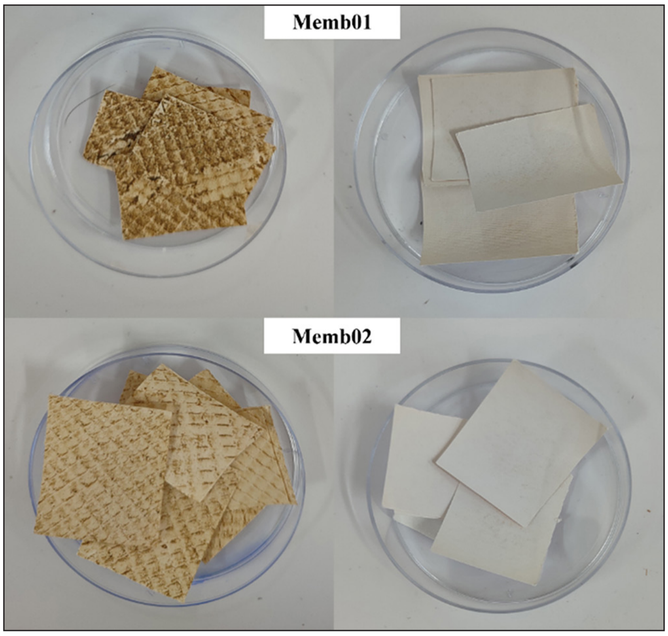

Figure 13. Membrane coupons before and after sequential cleaning showing removal of fouling material

SDS (10 mM, pH = 11), EDTA (1 mM, pH = 11), H_2O_2 (1 M, pH = 11), and sulfuric acid (pH = 4). The sequence was applied as shown in Fig. 12.

Figure 13 illustrates the significant improvement in membrane surface cleanliness after sequential cleaning. Nearly all fouling material was removed, with an average weight loss of 15% for Memb01 and 14% for Memb02. After optimizing chemical cleaning at the laboratory scale, future research will focus on scaling up the process using a pilot system.

CONCLUSIONS

Our study aimed to evaluate the fouling state of two used membranes taken from a desalination plant located in the province of Aïn Témouchent, Algeria. The investigation into the nature of the fouling products and the surfaces of the two fouled SWRO membranes was conducted to determine the type of fouling on the membrane surfaces and to establish an effective cleaning protocol. This is the first time such a study has been undertaken for Algerian reverse osmosis desalination plants. The physicochemical, morphological, and structural analysis of the polyamide-based surface material required several techniques (SEM-EDS, FTIR, XRD, and XRF). The membrane autopsies revealed the formation of an organo-inorganic complex on the surface layer of the membrane. Loss-on-ignition and calcimetry analysis indicated that the foulants contained over 30% OM and approximately 4% $CaCO_3$. FTIR-ATR analysis of the fouling material and membrane surfaces identified peaks corresponding to hydroxyl groups, phenolic compounds, amide bonds, and C–C bonds, suggesting the accumulation of organic substances such as proteins, humic substances, and possibly polysaccharides. Additionally, XRF, XRD, and EDS analysis revealed the presence of inorganic scale-forming compounds, primarily Na, Cl, Mg, Al, Si, K, Mo, Fe, and Ca. Diffraction techniques confirmed that the inorganic portion of the fouling material contained a significant amount of SiO_2, mainly of marine origin. Surface analysis of the fouled membrane samples using SEM-EDS confirmed the presence of a variety of inorganic chemical elements. Based on these results, it is recommended to effectively reduce fouling on the membrane surface by using a chemical cleaning protocol that includes alkaline NaOH, a metal chelating agent (EDTA), a surfactant (SDS), an oxidant (H_2O_2), followed by H_2SO_4 acid, with DI rinsing after each agent. This approach successfully removed almost all fouling materials from the membrane surface.

ACKNOWLEDGEMENTS

We thank the Thematic Research Agency in Science and Technology (ATRST) for its support. We are grateful to the Beni Saf Water Company (BWC) for facilitating sampling at the station. We also acknowledge the technical staff of the Center for Scientific and Technical Research in Physico-Chemical Analyses (CRAPC): M Boutaiba and N Yezli (CRAPC), A Bouchama (CRAPC–PTAPC Mostaganem), and H Boulahbal (CRAPC–PTAPC Ouargla), for conducting most of the analyses which significantly contributed to the outcomes of this study.

AUTHOR CONTRIBUTIONS

Abdessalam Radjai: conceptualization, formal analysis, investigation, methodology, visualization, writing original draft. Mourad Amara: investigation, methodology, conceptualization, validation, supervision. Fouzia Houma: project administration, resources. Hafida Hadjar: data curation, formal analysis, investigation, project administration, visualization, writing review and editing. Safia Chernai: supervision, writing original draft. Saifi Amirouche: formal analysis. Boualem Hamdi: conceptualization, investigation, methodology, project administration, validation, supervision, visualization, writing original draft.

ORCID

Abdessalam Radjai
https://orcid.org/0000-0001-7999-0331

REFERENCES

ADEL M, NADA T, AMIN S, ANWAR T and MOHAMED AA (2022) Characterization of fouling for a full-scale seawater reverse osmosis plant on the Mediterranean sea: membrane autopsy and chemical cleaning efficiency. *Groundw. Sustain. Dev.* **16**. https://doi.org/10.1016/j.gsd.2021.100704

AFNOR (1996) NF P 94-048. AFNOR, Paris. 11 pp.

AHMED MA, AMIN S and MOHAMED AA (2023) Fouling in reverse osmosis membranes: monitoring, characterization, mitigation strategies and future directions. *Heliyon* **9** (4). https://doi.org/10.1016/j.heliyon.2023.e14908

AL ASHHAB A, SWEITY A, BAYRAMOGLU B, HERZBERG M and GILLOR O (2017) Biofouling of reverse osmosis membranes: effects of cleaning on biofilm microbial communities, membrane performance, and adherence of extracellular polymeric substances. *Biofouling* **33** (5) 397–409. https://doi.org/10.1080/08927014.2017.1318382

AL-ABRI M, KYAW HH, AL-GHAFRI B, MYINT MTZ and DOBRETSOV S (2022) Autopsy of used reverse osmosis membranes from the largest seawater desalination plant in Oman. *Membranes* **12** (7) 671. https://doi.org/10.3390/membranes12070671

AL-AMOUDI A and LOVITT RW (2007) Fouling strategies and the cleaning system of NF membranes and factors affecting cleaning efficiency. *J. Membr. Sci.* **303** (1–2) 4–28. https://doi.org/10.1016/J.MEMSCI.2007.06.002

AL-SAIDI M, BIRNBAUM D, BURITI R, DIEK E, HASSELBRING C, JIMENEZ A and WOINOWSKI D (2016) Water resources vulnerability assessment of MENA countries considering energy and virtual water interactions. *Proced. Eng.* **145** 900–907. https://doi.org/10.1016/j.proeng.2016.04.117

AMITOUCHE M and REMINI B (2016) Operation of Cap Djinet desalination plant and dilution of brine with power station cooling water. *Desalination Water Treat.* **57** (8) 3514–3521. https://doi.org/10.1080/19443994.2014.987824

ANG WS, LEE S and ELIMELECH M (2006) Chemical and physical aspects of cleaning of organic-fouled reverse osmosis membranes. *J. Membr. Sci.* **272** (1–2) 198–210. https://doi.org/10.1016/j.memsci.2005.07.035

ASHFAQ MY, AL-GHOUTI MA, QIBLAWEY H and ZOUARI N (2019) Evaluating the effect of antiscalants on membrane biofouling using FTIR and multivariate analysis. *Biofouling* **35** (1) 1–14. https://doi.org/10.1080/08927014.2018.1557637

BAIZE D (2018) *Guide des Analyses en Pédologie* 3rd edn). Editions Quae, Paris. 328 pp.

BUTT FH, RAHMAN F and BADURUTHAMAL U (1997) Characterization of foulants by autopsy of RO desalination membranes. *Desalination* **114** (1) 51–64. https://doi.org/10.1016/S0011-9164(97)00154-9

CHOI YH, KWEON JH, KIM DI and LEE S (2009) Evaluation of various pretreatment for particle and inorganic fouling control on performance of SWRO. *Desalination* **247** (1–3) 137–147. https://doi.org/10.1016/j.desal.2008.12.019

CREBER SA, VROUWENVELDER JS, VAN LOOSDRECHT MCM and JOHNS ML (2010) Chemical cleaning of biofouling in reverse osmosis membranes evaluated using magnetic resonance imaging. *J. Membr. Sci.* **362** (1–2) 202–210. https://doi.org/10.1016/J.MEMSCI.2010.06.052

DÍAZ SALAZAR JF and GORCZYCA B (2024) Mechanism of nanofiltration fouling in high hardness and dissolved organic carbon surface water based on chemical characterization of foulant. *Desalination Water Treat.* **320**. https://doi.org/10.1016/j.dwt.2024.100838

FAN C, YAN J, LIU H, XIE Y and LIU H (2024) Performance and membrane fouling characteristics of a drinking water multistage NF system based on membrane autopsy from a full-scale system. *J. Water Proc. Eng.* **58**. https://doi.org/10.1016/j.jwpe.2024.104909

FILLOUX E, WANG J, PIDOU M, GERNJAK W and YUAN Z (2015) Biofouling and scaling control of reverse osmosis membrane using one-step cleaning-potential of acidified nitrite solution as an agent. *J. Membr. Sci.* **495** 276–283. https://doi.org/10.1016/j.memsci.2015.08.034

FLEMMING HC (1997) Reverse osmosis membrane biofouling. *Exp. Therm. Fluid Sci.* **14** (4) 382–391. https://doi.org/10.1016/S0894-1777(96)00140-9

FONTYN M, VAN 'T RIET K and BIJSTERBOSCH BH (1991) Surface spectroscopic studies of pristine and fouled membranes Part 1. Method development and pristine membrane characterization. *Colloids Surf.* **54** 331–347. https://doi.org/10.1016/0166-6622(91)80072-V

FORTUNATO L, ALSHAHRI AH, FARINHA ASF, ZAKZOUK I, JEONG S and LEIKNES TO (2020) Fouling investigation of a full-scale seawater reverse osmosis desalination (SWRO) plant on the Red Sea: Membrane autopsy and pretreatment efficiency. *Desalination* **496**. https://doi.org/10.1016/j.desal.2020.114536

FU H, JIAN X, ZHANG W and SHANG F (2020) A comparative study of methods for determining carbonate content in marine and terrestrial sediments. *Mar. Petrol. Geol.* **116**. https://doi.org/10.1016/j.marpetgeo.2020.104337

GAN Q, HOWELL JA, FIELD RW, ENGLAND R, BIRD MR and MCKECHINIE MT (1999) Synergetic cleaning procedure for a ceramic membrane fouled by beer microfiltration. *J. Membr. Sci.* **155** (2) 277–289. https://doi.org/10.1016/S0376-7388(98)00320-2

GAO S, CUI X and ZHANG S (2020) Utilization of molybdenum tailings in concrete manufacturing: A review. *Appl. Sci.* **10** (1). https://doi.org/10.3390/app10010138

GLEICK PH (2014) *The World's Water Volume 8*. Island Press, Washington, DC. 476 pp.

GOH PS, LAU WJ, OTHMAN MHD and ISMAIL AF (2018) Membrane fouling in desalination and its mitigation strategies. *Desalination* **425** 130–155. https://doi.org/10.1016/j.desal.2017.10.018

GUL A, HRUZA J and YALCINKAYA F (2021) Fouling and chemical cleaning of microfiltration membranes: A mini-review. *Polymers* **13** (6). https://doi.org/10.3390/polym13060846

GUO H, TANG X, GANSCHOW G and KORSHIN G V. (2019) Differential ATR FTIR spectroscopy of membrane fouling: Contributions of the substrate/fouling films and correlations with transmembrane pressure. *Water Res.* **161** 27–34. https://doi.org/10.1016/j.watres.2019.05.086

HANSIMA MACK, JAYAWEERA AT, KETHARANI J, RITIGALA T, ZHENG L, SAMARAJEEWA DR, NANAYAKKARA KGN, HERATH AC, MAKEHELWALA M, JINADASA KBSN and co-authors (2022) Characterization of humic substances isolated from a tropical zone and their role in membrane fouling. *J. Environ. Chem. Eng.* **10** (3). https://doi.org/10.1016/j.jece.2022.107456

HASANZADEH R, SOURAKI BA and PENDASHTEH A (2023) Insights into the foulants characteristics in a walnut shell biofilm-membrane bioreactor during treatment of hypersaline oilfield produced water. *J. Water Process. Eng.* **54**. https://doi.org/10.1016/j.jwpe.2023.104011

HEIRI O, LOTTER AF and LEMCKE G (2001) Loss on ignition as a method for estimating organic and carbonate content in sediments: Reproducibility and comparability of results. *J. Paleolimnol.* **25** (1) 101–110. https://doi.org/10.1023/A:1008119611481

HONG S and ELIMELECH M (1997) Chemical and physical aspects of natural organic matter (NOM) fouling of nanofiltration membranes. *J. Membr. Sci.* **132** (2) 159–181. https://doi.org/10.1016/S0376-7388(97)00060-4

HUSSEIN AL-TIMIMI DA, ALSALHY QF, ABDULRAZAK AA and DRIOLI E (2022) Novel polyether sulfone/polyethylenimine grafted nano-silica nanocomposite membranes: Interaction mechanism and ultrafiltration performance. *J. Membr. Sci.* **659**. https://doi.org/10.1016/j.memsci.2022.120784

JAWOR A and HOEK EMV (2009) Effects of feed water temperature on inorganic fouling of brackish water RO membranes. *Desalination* **235** (1–3) 44–57. https://doi.org/10.1016/J.DESAL.2008.07.004

HYDRANAUTICS (2014) Foulants and cleaning procedures for composite polyamide RO membrane elements (ESPA, ESNA, CPA, LFC, NANO and SWC). Hydranautics, Oceanside, California. 16 pp.

JORA (Official Journal of the Algerian Republic) (2023) Executive Decree No. 23-103 of 7 March 2023 on the creation, organisation and functioning of the National Water Desalination Agency. JORA, Algiers, Algeria. 24 pp.

JUNG J, RYU JH, CHOI SY, PARK KY, SONG WJ, YU YJ, JANG Y-S, PARK J and KWEON J (2018) Autopsy study of irreversible foulants on polyvinylidene fluoride hollow-fiber membranes in an immersed microfiltration system operated for five years. *Sep. Purif. Technol.* **199** 1–8. https://doi.org/10.1016/j.seppur.2018.01.039

KABATA-PENDIAS A and MUKHERJEE AB (2007) *Trace Elements from Soil to Human*. Springer, Berlin. 550 pp. https://doi.org/10.1007/978-3-540-32714-1

KARMAL I, MOHAREB S, EL HOUSSE M, HAFID N, HADFI A, BELATTAR M, BEN-AAZZA S, ADDI AA, AKBOUR RA, HAMDANI M and co-authors (2020) Structural and morphological characterization of scale deposits on the reverse osmosis membranes: Case of brackish water demineralization station in Morocco. *Groundwater Sust. Dev.* **11**. https://doi.org/10.1016/j.gsd.2020.100483

KHALIL AKA, ELGAMOUZ A, NAZIR S, ATIEH MA, ALAWADHI H and LAOUI T (2024) Preparation and characterization of clay based ceramic porous membranes and their use for the removal of lead ions from synthetic wastewater with an insight into the removal mechanism. *Heliyon* **10** (3). https://doi.org/10.1016/j.heliyon.2024.e24939

KHAMIS F and ARAFAH D (2017) Thermoluminescence characteristics of natural quartz and synthesized silica glass prepared by sol-gel technique. *Asian J. Phys. Chem. Sci.* **3** (1) 1–16. https://doi.org/10.9734/ajopacs/2017/35542

KHAN MT, BUSCH M, MOLINA VG, EMWAS AH, AUBRY C and CROUE JP (2014) How different is the composition of the fouling layer of wastewater reuse and seawater desalination RO membranes? *Water Res.* **59** 271–282. https://doi.org/10.1016/j.watres.2014.04.020

KHOO YS, LAU WJ, HASAN SW, SALLEH WNW and ISMAIL AF (2021) New approach of recycling end-of-life reverse osmosis membranes via sonication for microfiltration process. *J. Environ. Chem. Eng.* **9** (6). https://doi.org/10.1016/j.jece.2021.106731

KRAMER CJM and DUINKER JC (1984) Complexation of trace metals in natural waters. In: *Proceedings of the International Symposium*, 2–6 May 1983, Texel, the Netherlands. https://doi.org/10.1007/978-94-009-6167-8

KUSANGAYA S, WARBURTON ML, ARCHER VAN GARDEREN E and JEWITT GPW (2014) Impacts of climate change on water resources in southern Africa: A review. *Phys. Chem. Earth* **67–69** 47–54. https://doi.org/10.1016/j.pce.2013.09.014

LAMSAL R, HARROUN SG, BROSSEAU CL and GAGNON GA (2012) Use of surface enhanced Raman spectroscopy for studying fouling on nanofiltration membrane. *Sep. Purif. Technol.* **96** 7–11. https://doi.org/10.1016/j.seppur.2012.05.019

LAQBAQBI M, SANMARTINO JA, KHAYET M, GARCÍA-PAYO C and CHAOUCH M (2017) Fouling in membrane distillation, osmotic distillation and osmotic membrane distillation. *Appl. Sci.* **7** (4). https://doi.org/10.3390/app7040334

LEAL FILHO W, TOTIN E, FRANKE JA, ANDREW SM, ABUBAKAR IR, AZADI H, NUNN PD, OUWENEEL B, WILLIAMS PA and SIMPSON NP (2022) Understanding responses to climate-related water scarcity in Africa. *Sci. Total. Environ.* **806**. https://doi.org/10.1016/j.scitotenv.2021.150420

LEE YG, KIM S, SHIN J, RHO H, KIM YM, CHO KH, EOM H, OH SE, CHO J and CHON K (2021) Sequential effects of cleaning protocols on desorption of reverse osmosis membrane foulants: Autopsy results from a full-scale desalination plant. *Desalination* **500**. https://doi.org/10.1016/j.desal.2020.114830

LEGER JP and HAWKER LC (1987) The composition and structure of reverse osmosis foulant deposits formed from rand water board water: A preliminary investigation. *Desalination* **61** (2) 137–158. https://doi.org/10.1016/0011-9164(87)80014-0

LIN JC-T, LEE DJ and HUANG C (2010) Membrane fouling mitigation: Membrane cleaning. *Sep. Sci. Technol.* **45** (7) 858–872. https://doi.org/10.1080/01496391003666940

LIU D, ZHU J, QIU M and HE C (2016) Antifouling performance of poly(lysine methacrylamide)-grafted PVDF microfiltration membrane for solute separation. *Sep. Purif. Technol.* **171** 1–10. https://doi.org/10.1016/J.SEPPUR.2016.07.006

LIU W, XIA R, LIN X, WANG Z, ANSARI AJ, LI G and LUO W (2024) Tracking fouling layer formation in membrane distillation of landfill leachate concentrate: Insights from periodic membrane autopsies. *J. Membr. Sci.* **693**. https://doi.org/10.1016/j.memsci.2023.122331

LIU Y, ZHANG S and WANG G (2013) The preparation of antifouling ultrafiltration membrane by surface grafting zwitterionic polymer onto poly(arylene ether sulfone) containing hydroxyl groups membrane. *Desalination* **316** 127–136. https://doi.org/10.1016/j.desal.2013.02.004

MADAENI SS and SAMIEIRAD S (2010) Chemical cleaning of reverse osmosis membrane fouled by wastewater. *Desalination* **257** (1–3) 80–86. https://doi.org/10.1016/j.desal.2010.03.002

MAHMOUDI A, BOSTANI M, RASHIDI S and VALIPOUR MS (2023) Challenges and opportunities of desalination with renewable energy resources in Middle East countries. *Renew. Sustain. Energy Rev.* **184**. https://doi.org/10.1016/j.rser.2023.113543

MARTIN KJ, BOLSTER D, DERLON N, MORGENROTH E and NERENBERG R (2014) Effect of fouling layer spatial distribution on permeate flux: A theoretical and experimental study. *J. Membr. Sci.* **471** 130–137. https://doi.org/10.1016/J.MEMSCI.2014.07.045

MATIN A, KHAN Z, ZAIDI SMJ and BOYCE MC (2011) Biofouling in reverse osmosis membranes for seawater desalination: Phenomena and prevention. *Desalination* **281** 1–16. https://doi.org/10.1016/J.DESAL.2011.06.063

MATIN A, RAHMAN F, SHAFI HZ and ZUBAIR SM (2019) Scaling of reverse osmosis membranes used in water desalination: Phenomena, impact, and control; future directions. *Desalination* **455** 135–157. https://doi.org/10.1016/J.DESAL.2018.12.009

MELIÁN-MARTEL N, SADHWANI JJ, MALAMIS S and OCHSENKÜHN-PETROPOULOU M (2012) Structural and chemical characterization of long-term reverse osmosis membrane fouling in a full scale desalination plant. *Desalination* **305** 44–53. https://doi.org/10.1016/j.desal.2012.08.011

MOKHTARI S, RAHIMPOUR A, SHAMSABADI AA, HABIBZADEH S and SOROUSH M (2017) Enhancing performance and surface antifouling properties of polysulfone ultrafiltration membranes with salicylate-alumoxane nanoparticles. *Appl. Surf. Sci.* **393** 93–102. https://doi.org/10.1016/j.apsusc.2016.10.005

NYSTRÖM M, RUOHOMÄKI K and KAIPIA L (1996) Humic acid as a fouling agent in filtration. *Desalination* **106** (1–3) 79–87. https://doi.org/10.1016/S0011-9164(96)00095-1

ONS (National Statistics Office, Algeria) (2024) National Statistics Office. URL: https://www.ons.dz/ (Accessed 16 October 2024).

PAN Y, XU R, LÜ Z, YU S, LIU M and GAO C (2017) Enhanced both perm-selectivity and fouling resistance of poly(piperazine-amide) nanofiltration membrane by incorporating sericin as a co-reactant of aqueous phase. *J. Membr. Sci.* **523** 282–290. https://doi.org/10.1016/j.memsci.2016.10.011

PAUL SK and NAIDU R (2022) Layered aluminosilicate nanoskeletons: The structure and properties of nanoherbicide formulations. *Adv. Agron.* **175** 301–345. https://doi.org/10.1016/BS.AGRON.2022.04.003

PHILIBERT M, VILLACORTE LO, EKOWATI Y, ABUSHABAN A and SALINAS-RODRIGUEZ SG (2024) Fouling and scaling in reverse osmosis desalination plants: A critical review of membrane autopsies, feedwater quality guidelines and assessment methods. *Desalination* **592**. https://doi.org/10.1016/j.desal.2024.118188

PIHLAJAMÄKI A, VÄISÄNEN P and NYSTRÖM M (1998) Characterization of clean and fouled polymeric ultrafiltration membranes by Fourier transform IR spectroscopy–attenuated total reflection. *Colloids Surf. A Physicochem. Eng. Asp.* **138** (2–3) 323–333. https://doi.org/10.1016/S0927-7757(96)03883-6

PORCELLI N and JUDD S (2010) Chemical cleaning of potable water membranes: A review. *Sep. Purif. Technol.* **71** (2) 137–143. https://doi.org/10.1016/j.seppur.2009.12.007

PULYALINA A, TIAN N, SENCHUKOVA A, FAYKOV I, RYABIKOVA M, NOVIKOV A, SAPRYKINA N and POLOTSKAYA G (2022) Application of cyclized polyacrylonitrile for ultrafiltration membrane fouling mitigation. *Membranes* **12** (5). https://doi.org/10.3390/membranes12050489

REN PF, FANG Y, WAN LS, YE XY and XU ZK (2015) Surface modification of polypropylene microfiltration membrane by grafting poly(sulfobetaine methacrylate) and poly(ethylene glycol): Oxidative stability and antifouling capability. *J. Membr. Sci.* **492** 249–256. https://doi.org/10.1016/j.memsci.2015.05.029

SAHADAT HOSSAIN M, JAHAN SA and AHMED S (2023) Crystallographic characterization of bio-waste material originated $CaCO_3$, green-synthesized CaO and $Ca(OH)_2$. *Results Chem.* **5**. https://doi.org/10.1016/j.rechem.2023.100822

SAKINAH AMM, ISMAIL AF, ILLIAS RM and HASSAN O (2007) Fouling characteristics and autopsy of a PES ultrafiltration membrane in cyclodextrins separation. *Desalination* **207** (1–3) 227–242. https://doi.org/10.1016/j.desal.2006.08.007

SAYED ET, OLABI AG, ELSAID K, AL RADI M, ALQADI R and ALI ABDELKAREEM M (2023) Recent progress in renewable energy based-desalination in the Middle East and North Africa MENA region. *J. Adv. Res.* **48** 125–156. https://doi.org/10.1016/j.jare.2022.08.016

SHAFI HZ, MATIN A, AKHTAR S, GLEASON KK, ZUBAIR SM and KHAN Z (2017) Organic fouling in surface modified reverse osmosis membranes: Filtration studies and subsequent morphological and compositional characterization. *J. Membr. Sci.* **527** 152–163. https://doi.org/10.1016/j.memsci.2017.01.017

SMITH B (2018) *Infrared Spectral Interpretation: A Systematic Approach*. CRC Press, Boca Raton. 288 pp. https://doi.org/10.1201/9780203750841

SOULA R, CHEBIL A, MCCANN L and MAJDOUB R (2021) Water scarcity in the Mahdia region of Tunisia: Are improved water policies needed? *Groundwater Sust. Dev.* **12**. https://doi.org/10.1016/j.gsd.2020.100510

TAPIERO Y, MERY F and GARCÍA A (2023) Understanding of surface fouling of brackish water reverse osmosis spiral wound membrane using an integrated analysis of seawater quality and membrane autopsy. *Chem. Eng. Sci.* **280**. https://doi.org/10.1016/j.ces.2023.119028

THUVANDER J, ZAREBSKA A, HÉLIX-NIELSEN C and JÖNSSON AS (2018) Characterization of irreversible fouling after ultrafiltration of thermomechanical pulp mill process water. *J. Wood Chem. Technol.* **38** (3) 276–285. https://doi.org/10.1080/02773813.2018.1454962

THYGESEN O, HEDEGAARD MAB, ZAREBSKA A, BELEITES C and KRAFFT C (2014) Membrane fouling from ammonia recovery analysed by ATR-FTIR imaging. *Vib. Spectrosc.* **72** 119–123. https://doi.org/10.1016/j.vibspec.2014.03.004

TRAN T, BOLTO B, GRAY S, HOANG M and OSTARCEVIC E (2007) An autopsy study of a fouled reverse osmosis membrane element used in a brackish water treatment plant. *Water Res.* **41** (17) 3915–3923. https://doi.org/10.1016/j.watres.2007.06.008

TZOTZI C, PAHIADAKI T, YIANTSIOS SG, KARABELAS AJ and ANDRITSOS N (2007) A study of CaCO3 scale formation and inhibition in RO and NF membrane processes. *J. Membr. Sci.* 296 (1–2) 171–184. https://doi.org/10.1016/j.memsci.2007.03.031

UNAL BO (2022) Membrane autopsy study to characterize fouling type of RO membrane used in an industrial zone wastewater reuse plant. *Desalination* **529**. https://doi.org/10.1016/j.desal.2022.115648

VEERASAMY D and ISMAIL AF (2012) Rehabilitation of fouled membrane from natural rubber skim latex concentration through membrane autopsy and ultrasonication enhanced membrane cleaning procedure. *Desalination* **286** 235–241. https://doi.org/10.1016/j.desal.2011.11.028

WANG Z, TANG J, ZHU C, DONG Y, WANG Q and WU Z (2015) Chemical cleaning protocols for thin film composite (TFC) polyamide forward osmosis membranes used for municipal wastewater treatment. *J. Membr. Sci.* **475** 184–192. https://doi.org/10.1016/j.memsci.2014.10.032

WU J, WANG Z, WANG Y, YAN W, WANG J and WANG S (2015) Polyvinylamine-grafted polyamide reverse osmosis membrane with improved antifouling property. *J. Membr. Sci.* **495** 1–13. https://doi.org/10.1016/j.memsci.2015.08.007

YANG H, YE S, WANG J, WANG H, WANG Z, CHEN Q, WANG W, XIANG L, ZENG G and TAN X (2021) The approaches and prospects for natural organic matter-derived disinfection byproducts control by carbon-based materials in water disinfection progresses. *J. Clean. Prod.* **311**. https://doi.org/10.1016/J.JCLEPRO.2021.127799

ZHENG L, YU D, WANG G, YUE Z, ZHANG C, WANG Y, ZHANG J, WANG J, LIANG G and WEI Y (2018) Characteristics and formation mechanism of membrane fouling in a full-scale RO wastewater reclamation process: Membrane autopsy and fouling characterization. *J. Membr. Sci.* **563** 843–856. https://doi.org/10.1016/j.memsci.2018.06.043

ZLATI ML, ANTOHI VM, IONESCU RV, ITICESCU C and GEORGESCU LP (2024) Quantifying the impact of the water security index on socio-economic development in EU27. *Socio-Econ. Plann. Sci.* **93**. https://doi.org/10.1016/j.seps.2024.101912

APPENDIX

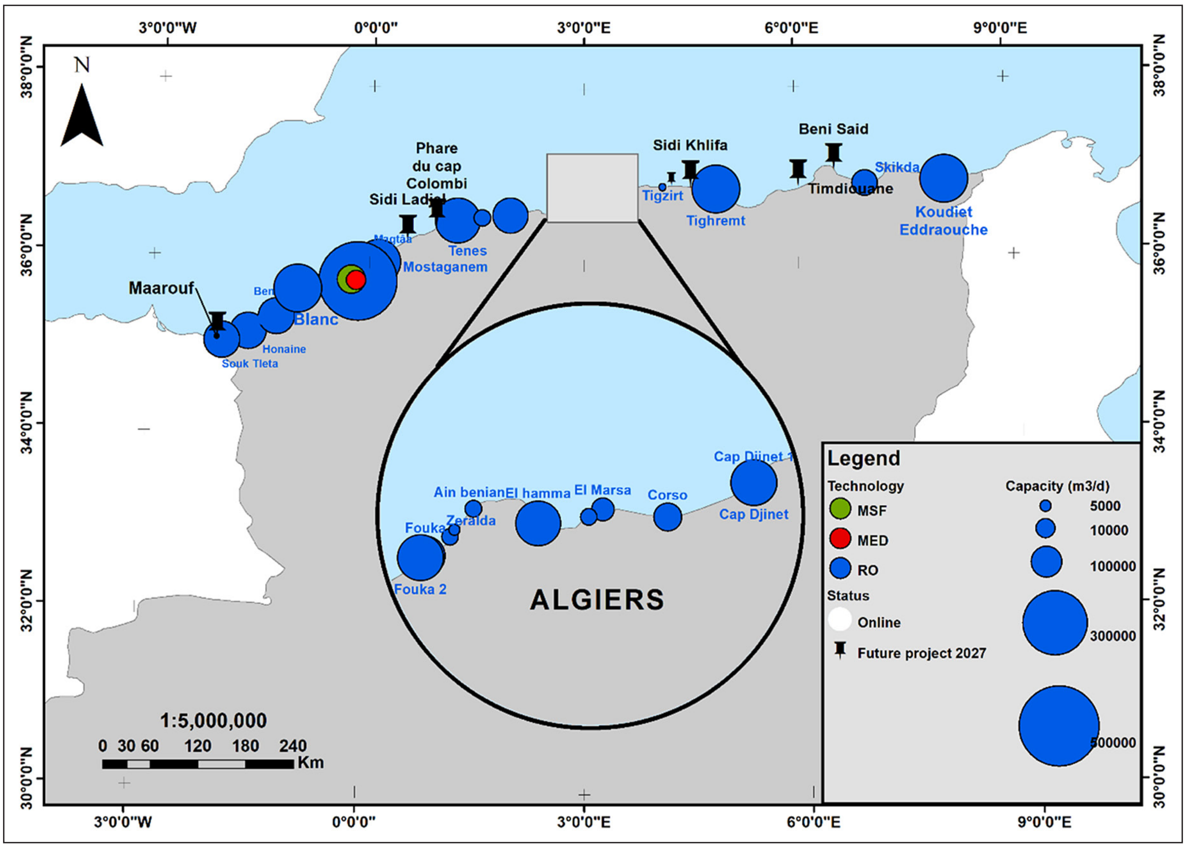

Figure A1. Mapping of desalination plants in Algeria